ELSEVIER

Journal of Alloys and Compounds 444–445 (2007) 606–609

Journal of ALLOYS AND COMPOUNDS

www.elsevier.com/locate/jallcom

Structural characterization of Pu-bearing murataite ceramic

S.V. Yudintsev [a], S.V. Stefanovsky [b,*], B.S. Nikonov [a], K.I. Maslakov [c], A.G. Ptashkin [b]

[a] *Institute of Geology of Ore Deposits RAS, Staromonetni 35, Moscow 109017, Russia*
[b] *SIA Radon, 7th Rostovskii Lane 2/14, Moscow 119121, Russia*
[c] *RRC "Kurchatov Institute", Kurchatov Sq. 1, Moscow, Russia*

Received 3 July 2006; received in revised form 30 September 2006; accepted 31 October 2006
Available online 30 November 2006

Abstract

Phase composition of the murataite ceramic containing 10 wt.% PuO_2 and oxidation states of the elements composing this ceramic have been studied. The ceramic is composed of three murataite polytypes with five-, eight-, and three-fold fluorite unit cell forming core, intermediate zone and rim of the murataite grains and minor crichtonite. Manganese, iron, and plutonium exist mainly in di-, tri-, and tetravalent forms, respectively.

Keywords: Ceramics; Scanning electron microscopy (SEM); Transmission electron microscopy (TEM); X-ray photoelectron spectroscopy; X-ray diffraction

1. Introduction

Murataite is considered as a promising host phase for actinides and rare earths as well as corrosion products and process contaminants in high level waste (HLW) and, therefore, murataite-based ceramics may be perspective for immobilization of complex actinide-containing wastes such as actinide or actinide/rare earth fractions of HLW [1,2]. Murataite as well as pyrochlore has a fluorite-derived structure [2–4]. In general, pyrochlore, $A^{VIII}{}_2B^{VI}{}_2O_{7-x}$ ($A = REE^{3+}$, $An^{3+/4+}$, Ca^{2+}; $B = Ti^{4+}$, Zr^{4+}, Hf^{4+}) and murataite, $A^{VIII}{}_3B^{VI}{}_6C^{V}{}_2O_{20-x}$ ($A = REE^{3+/4+}$, $An^{3+/4+}$, Zr^{4+}, Ca^{2+}, Na^{+}; $B = Ti^{4+}$, Fe^{3+}, $Mn^{3+/4+}$, Al^{3+}; $C = Mn^{2+}$, Fe^{2+}) being structure-related compounds form a polysomatic series of the phases with modular structure and two- (2C pyrochlore), three- (3C murataite), five- (5C), seven- (7C), and eight-fold (8C) elementary fluorite unit cell [5]. All the phases with three-fold elementary fluorite unit cell and higher multiplicity, i.e. containing murataite modules in their structure are considered as murataite polytypes. The murataite structure contains four distinct cation sites capable to accommodate variable size cations [6]. Suitability of the murataite-based ceramics as potential nuclear waste forms was also confirmed by their good radiation resistance [7,8].

Previously we synthesized and examined Pu-bearing murataite-based ceramics [9–12]. In the present work the Pu-bearing murataite ceramic is characterized in more details in particular using X-ray photoelectron spectroscopy (XPS).

2. Experimental

The murataite ceramic with specified composition (wt.%): 5 Al_2O_3, 10 CaO, 55 TiO_2, 10 MnO, 5 Fe_2O_3, 5 ZrO_2, 10 PuO_2 was prepared by melting in air of oxide mixtures in a platinum ampoule at 1500 °C for 3 h followed by quenching. The sample was characterized with X-ray diffraction (XRD) using a DRON-4 diffractometer (Cu Kα radiation), scanning electron microscopy – energy dispersive system (SEM/EDS) using a JSM-5300 + Link ISIS unit, and transmission electron microscopy (TEM) – selected area electron diffraction (SAED) using a JEM-100c + KEVEX-5100 unit. XPS spectra were measured with an electrostatic spectrometer MK II VG Scientific using Al Kα and Mg Kα radiation under 1.3×10^{-7} Pa at a room temperature. Electron binding energies E_b (eV) were measured relatively to the binding energy of the C 1s electrons from hydrocarbons absorbed on the sample surface accepted to be equal to 285.0 eV.

3. Results

According to the XRD, SEM/EDS, and TEM/SAED data, the murataite ceramic is composed of predominant murataite-type phases: 5C, 8C and 3C, and minor crichtonite, also suggested as a waste form [13] (Figs. 1–3). Core of the murataite grains is composed of the 5C phase (the lightest on SEM-image) with the highest Pu content. The 8C phase with intermediate Pu content composes major bulk of the grains (light-gray). Rim is formed

* Corresponding author. Tel.: +7 495 919 3194.
E-mail address: profstef@mtu-net.ru (S.V. Stefanovsky).

0925-8388/$ – see front matter © 2006 Elsevier B.V. All rights reserved.
doi:10.1016/j.jallcom.2006.10.129

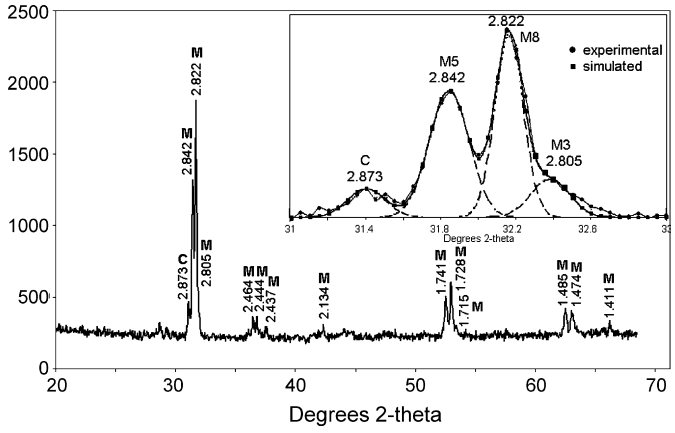

Fig. 1. XRD pattern of the Pu-doped murataite ceramic and computer simulation of major peak due to murataite (inset). M—murataite polytypes and C—crichtonite.

by the 3C phase (gray) with the lowest Pu content. Crichtonite (dark-gray) crystals contain traces of Pu.

The low binding energy XPS from murataite exhibits the outer valence molecular orbitals (OVMO) structure attributed to the outer Ca 4s, Pu 5f,7s, Zr 4d,5s, Fe 3d,4s, Ti 3d,4s, Mn 3d,4s, Al 3s,3p, and O 2p electrons, as well as the inner valence molecular orbitals (IVMO) structure due to the Ca 3s,3p, Pu 6s,6p, Zr 4p, Ti 3p, Mn 3p, and O 2s electrons (Fig. 4, Table 1). This binding energy range exhibits only the lines typical of the compounds studied. The Pu 4f spectrum of the sample exhibits the fine structure typical of the Pu^{4+} ions (Fig. 4) with the doublet split at $\Delta E_{sl} = 12.5$ eV. On the higher binding energy side from the basic peaks at $\Delta E_{sat} = 7.4$ eV the typical shake up satellite of about 19% intensity was observed. The oxidation states of the elements were determined to correspond to the following ions: Ca^{2+}, Ti^{4+}, Mn^{2+}, Fe^{3+}, Zr^{4+}, Al^{3+} and Pu^{4+}.

The O 1s spectrum consists of the two peaks at 530.0 and 532.1 eV. Taking into account equation $R_{M–O} = 2.27 (E_b - 519.4)^{-1}$, derived in [14], on the basis of the O 1s binding energy the interatomic distances $R_{M–O}$ (nm) calculated are 0.214 and 0.173 nm. As follows from this equation the O 1s binding energy decrease as the interatomic distance $R_{M–O}$ increases. Probably the value 0.173 nm can be attributed to the hydroxide groups on the surface of the sample. It agrees with the elemental analysis data indicating that the O 1s binding energy for Pu- and Np-bearing samples is the same. The value $R_{M–O} = 0.214$ nm corresponds to average M–O distance in the murataite structure [6].

4. Discussion

The phase composition and texture of the Pu-bearing murataite ceramic are typical of those for the murataite ceramics

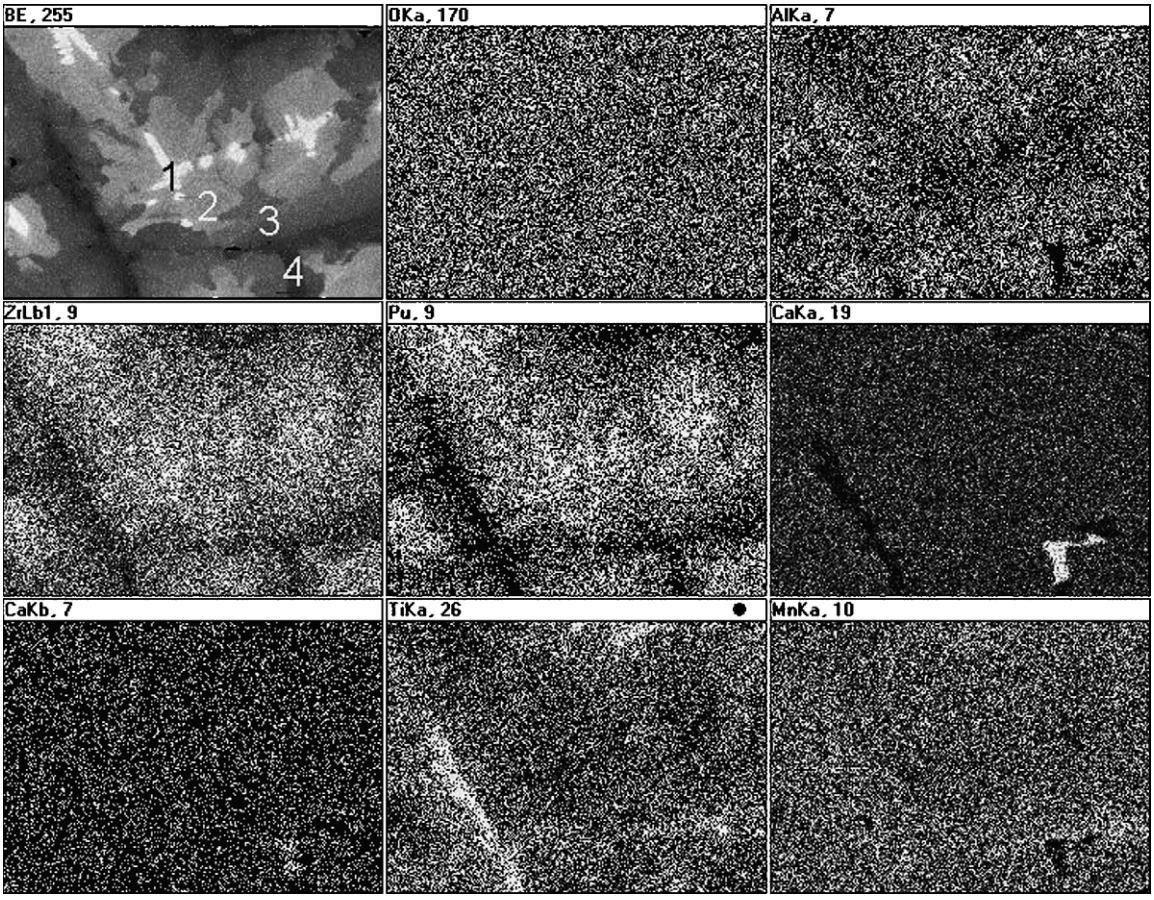

Fig. 2. SEM-image with X-ray mapping of the murataite ceramic 1, 2, 3 – 5C, 8C and 3C murataite polytypes, 4 – crichtonite.

Table 1
Binding energies E_b (eV) and FWHM values[a] (eV) of the outer (MO) and core electrons for the actinide-doped murataite ceramic

MO	Pu $4f_{7/2}$	Ca $2p_{3/2}$	Ti $2p_{3/2}$	Mn $2p_{3/2}$	Fe $2p_{3/2}$	Zr $3d_{5/2}$	Al 2p	O 1s
4.4; 22.0								530.0
24.7; 30.5	426.1	346.7	458.5	641.0	711.0	182.2	74.0	
36.9; 43.5	7.4 sat	(1.6)	(1.2)	(2.4)	(2.9)	(1.2)	(1.4)	532.1
48.3								(1.3)

[a] FWHM values are given in parentheses relative to the FWHM of the C 1s-peak accepted to be 1.3 eV. Initial C 1s FWHM for Pu-bearing murataite is 2.1 eV.

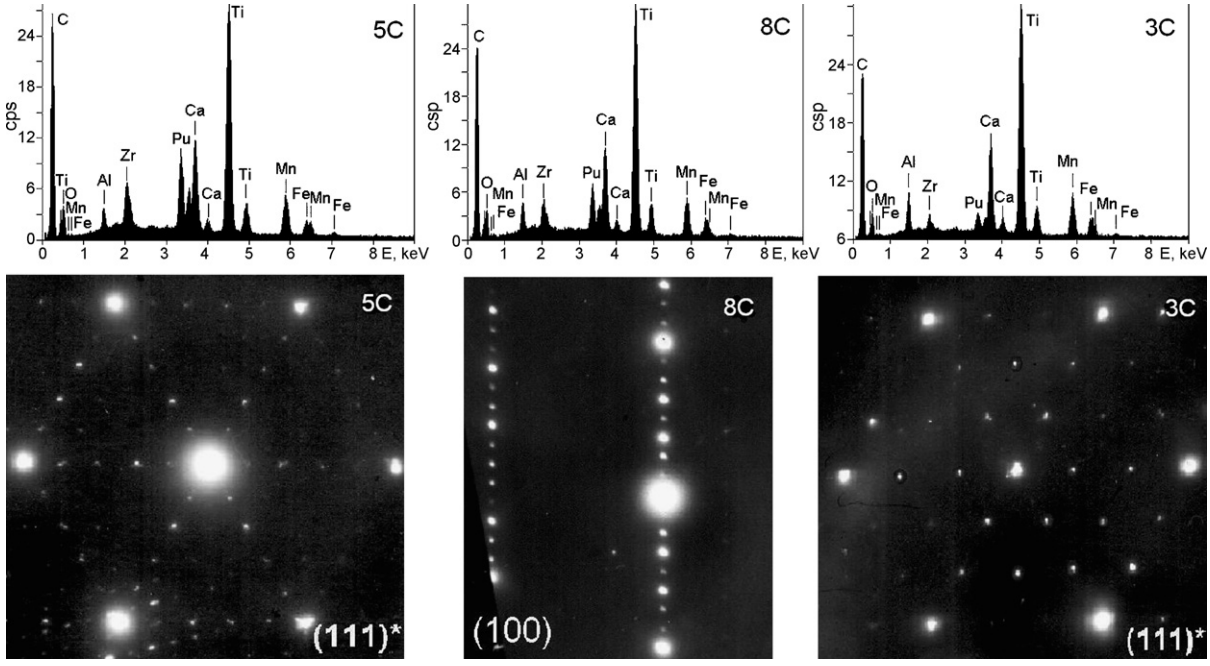

Fig. 3. EDX-spectra and SAED-patterns of the 5C, 8C, and 3C phases composing the murataite-based ceramic sample.

produced by melting and crystallization [1,2,9–12]. Such ceramics are composed of zoned murataite grains with increasing of the number of the murataite modules in the structure of the murataite polytypes from core to rim in the single grain. Because actinide content reduces in a series: 2C (pyrochlore) > 7C > 5C > 8C > 3C (murataite) [2,5] actinide depletion of the rim with respect to the core creates an additional barrier against their leaching by underground water and release into environment.

As follows from the XPS data such elements as Ca, Al, Ti, and Zr have their typical oxidation states—Ca^{2+}, Al^{3+}, Ti^{4+}, and Zr^{4+}. Transition elements—Mn and Fe were found to be mainly di- and trivalent, respectively. Occurrence of trivalent iron (Fe^{3+} ions) is consistent well with Mössbauer spectroscopy data [15]. However admixture of Mn(III), Mn(IV), and Fe(II) states may be also present. XANES data exhibit 60–70% of total Mn in a divalent and 20–30% in a trivalent form [16]. Pu was found to

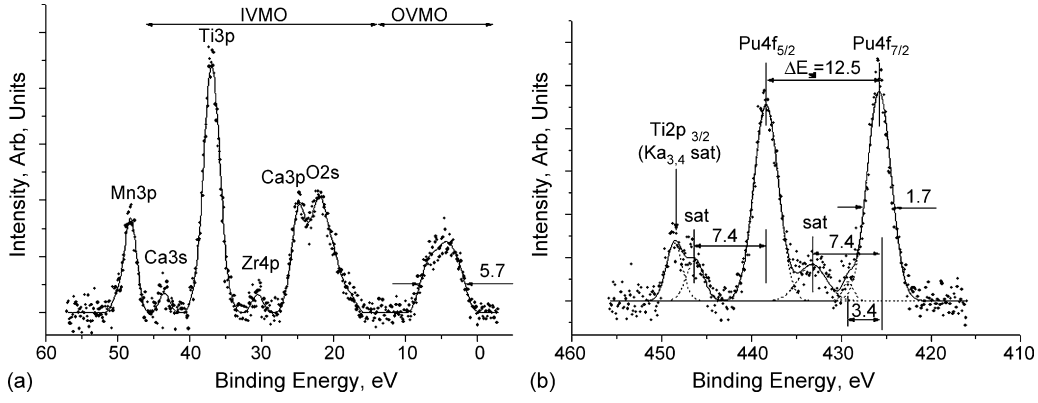

Fig. 4. Low binding energy (a) and Pu 4f (b) XPS from the murataite ceramic.

be in a tetravalent form due to oxidizing conditions of synthesis (melting in air atmosphere).

5. Conclusion

Murataite ceramic with specified chemical composition (wt.%): 5 Al_2O_3, 10 CaO, 55 TiO_2, 10 MnO, 5 Fe_2O_3, 5 ZrO_2, 10 PuO_2 produced by melting in air is composed of major murataite-type phases and minor crichtonite. Among the murataite-type phases varieties (polytypes) with five-, eight-, and three-fold fluorite unit cell forming core, intermediate zone, and rim of the murataite grains were found. Pu enters murataite phase and its concentration is the highest in the core of the murataite grains and reduces towards their rim. As follows from the XPS data, Pu exists in a tetravalent form, Mn is mainly divalent and Fe is trivalent. Other elements (Ca, Al, Ti, Zr) have their typical oxidation states.

Acknowledgement

The work was performed under financial support from Office of Basic Sciences of the US DOE (Project RUC2-20009-MO-04).

References

[1] S.V. Stefanovsky, S.V. Yudintsev, B.S. Nikonov, B.I. Omelianenko, A.G. Ptashkin, Mater. Res. Soc. Symp. Proc. 556 (1999) 121–128.
[2] S.V. Stefanovsky, S.V. Yudintsev, R. Gieré, G.R. Lumpkin, in: R. Gieré, P. Stille (Eds.), Energy, Waste, and the Environment: A Geological Perspective, Geological Society, London, 2004, pp. 37–63.
[3] J. Lian, S.V. Yudintsev, S.V. Stefanovsky, O.I. Kirjanova, R.C. Ewing, Mater. Res. Soc. Symp. Proc. 713 (2002) 455–460.
[4] R.C. Ewing, W.J. Weber, J. Lian, J. Appl. Phys. 95 (2004) 5949–5971.
[5] V.S. Urusov, N.I. Organova, O.V. Karimova, S.V. Yudintsev, S.V. Stefanovsky, Trans. (Doklady) Russ. Acad. Sci./Earth Sci. Sec. 401 (2005) 319–325.
[6] T.S. Ercit, F.C. Hawthorne, Canad. Miner. 33 (1995) 1223–1229.
[7] J. Lian, L.M. Wang, R.C. Ewing, S.V. Yudintsev, S.V. Stefanovsky, Mater. Res. Soc. Symp. Proc. 807 (2004) 225–230.
[8] J. Lian, L.M. Wang, R.C. Ewing, S.V. Yudintsev, S.V. Stefanovsky, J. Appl. Phys. 97 (2005) 113536.
[9] I.A. Sobolev, S.V. Stefanovsky, B.F. Myasoedov, Yu.M. Kuliako, S.V. Yudintsev, In: K.K.S. Pillay, K.C. Kim, (Eds.), Plutonium Future—The Science. Conf. Trans, AIP Conf. Proc. vol. 532, 2000, pp. 122–124.
[10] S.V. Yudintsev, S.V. Stefanovsky, B.I. Omelianenko, B.S. Nikonov, Mater. Res. Soc. Symp. Proc. 663 (2001) 357–366.
[11] S. Stefanovsky, O. Stefanovsky, S. Yudintsev, B. Nikonov, Proceedings of the 35th Journees des Actinides, Baden, Austria, April 23–26, 2005, Abstract E-19, CD-ROM.
[12] S.V. Stefanovsky, S.V. Yudintsev, B.S. Nikonov, S.A. Perevalov, O.I. Stefanovsky, A.G. Ptashkin, Mater. Res. Soc. Symp. Proc. 893 (2006), 893-JJ5-23.
[13] W.L. Gong, R.C. Ewing, L.M. Wang, H.S. Xie, Mater. Res. Soc. Symp. Proc. 353 (1995) 807–815.
[14] M.I. Sosulnikov, Yu.A. Teterin, Rep. Acad. Sci. USSR (Russ.) 317 (1991) 418–421.
[15] V.S. Urusov, V.S. Rusakov, S.V. Yudintsev, S.V. Stefanovsky, Mater. Res. Soc. Symp. Proc. 807 (2004) 243–248.
[16] S.V. Stefanovsky, S.V. Yudintsev, B.S. Nikonov, A.A. Shiryaev, V Conf. Radiochemistry-2006, Dubna, Russia, October 23–28, 2006. Abstracts, pp. 212–213.